Supporting Information

pH Titration Monitored by Quantum Cascade Laser-Based Vibrational Circular Dichroism

Anja Rüther,[1] Marcel Pfeifer,[2] Víctor A. Lórenz-Fonfría,[3] and Steffen Lüdeke[1]*

[1]Institute of Pharmaceutical Sciences, Albert-Ludwigs-Universität Freiburg, Albertstr. 25, 79104 Freiburg, Germany

[2]Fraunhofer Institute for Physical Measurement Techniques, Heidenhofstr. 8, 79110 Freiburg, Germany

[3]Experimental Molecular Biophysics, Freie Universität Berlin, Arnimallee 14, 14195 Berlin, Germany

Corresponding Author

*Dr. Steffen Lüdeke
Institute of Pharmaceutical Sciences
Albertstr. 25, D-79104 Freiburg, Gemany
E-mail: steffen.luedeke@pharmazie.uni-freiburg.de
Tel.: +49 (0)761 203-6353
Fax: +49 (0)761 203-6351

ANALYSIS OF EXPERIMENTAL DATA

The analysis of the three-dimensional data sets consisting of pH-dependent FT-IR, QCL-IR, or QCL-VCD spectra involved two steps: singular value decomposition (SVD) and global fitting. SVD and matrix operations were performed in MATLAB (MathWorks, Natick, MA, USA)

We arranged the pH-dependent spectra into a matrix **A** of size $m \times n$ with m being the number of wavenumbers in the corresponding experiment (FT-IR in the spectral range from 1800 to 1000 cm^{-1}: m = 493; FT-IR in the spectral range from 1320 to 1220 cm^{-1}: m = 57; QCL-IR and QCL-VCD in the spectral range from 1320 to 1220 cm^{-1}: m = 401) and n representing the number of pH values (FT-IR: n = 15; QCL-IR and QCL-VCD: n = 18). SVD delivered three matrices **U**, **S**, and **V** according to the decomposition $\mathbf{A} = \mathbf{U} \times \mathbf{S} \times \mathbf{V}^{\mathbf{T}}$. The columns of **U** ($m \times n$) contained the orthonormal spectra. Their associated orthonormal pH-titration vectors are the columns of **V** ($n \times n$). **S** ($n \times m$) is a diagonal matrix whose elements are known as the singular values. The singular values act as weights for the correct mixing of the columns of **U** and **V** to obtain **A** through matrix multiplication. Each pair of columns from **U** and **V** define an SVD component, arranged in decreasing order to describe the experimental data by least-squares. The number of significant SVD components, namely those containing signal-like spectra and pH-titration curves, indicates the estimated rank of the (ideal) data matrix, and therefore the estimated number of spectroscopically different chemical components present in the data set.

According to the matrix least-squares (MLS) method combined with SVD[1] the global fitting procedure was performed on the columns of **V**, which contained all information concerning the pH-dependence of the VCD data set. We fitted the columns of **V** to a two-pK Henderson–Hasselbalch equation with fixed pK values, solving $\mathbf{B} = \mathbf{F}^{+} \times \mathrm{S} \times \mathbf{V}$. $\mathbf{F}^{+}$ is the pseudoinverse of **F** ($n \times 3$), which is the matrix that includes the definition of the Henderson–Hasselbalch titration

profile (see eq. 3 in the manuscript). **B** (3×*n*) contains the estimated amplitudes of the model to fit each of the 18 columns of **V**. The matrix **D** (*m*×3), whose columns correspond to the spectra a_0, a_1, and a_2, was calculated as $\mathbf{D} = \mathbf{U}\times\mathbf{B}^{\mathbf{T}}$. Detailed background information on general applications of MLS combined with SVD for analysis of spectroscopic data can be found elsewhere.[2]

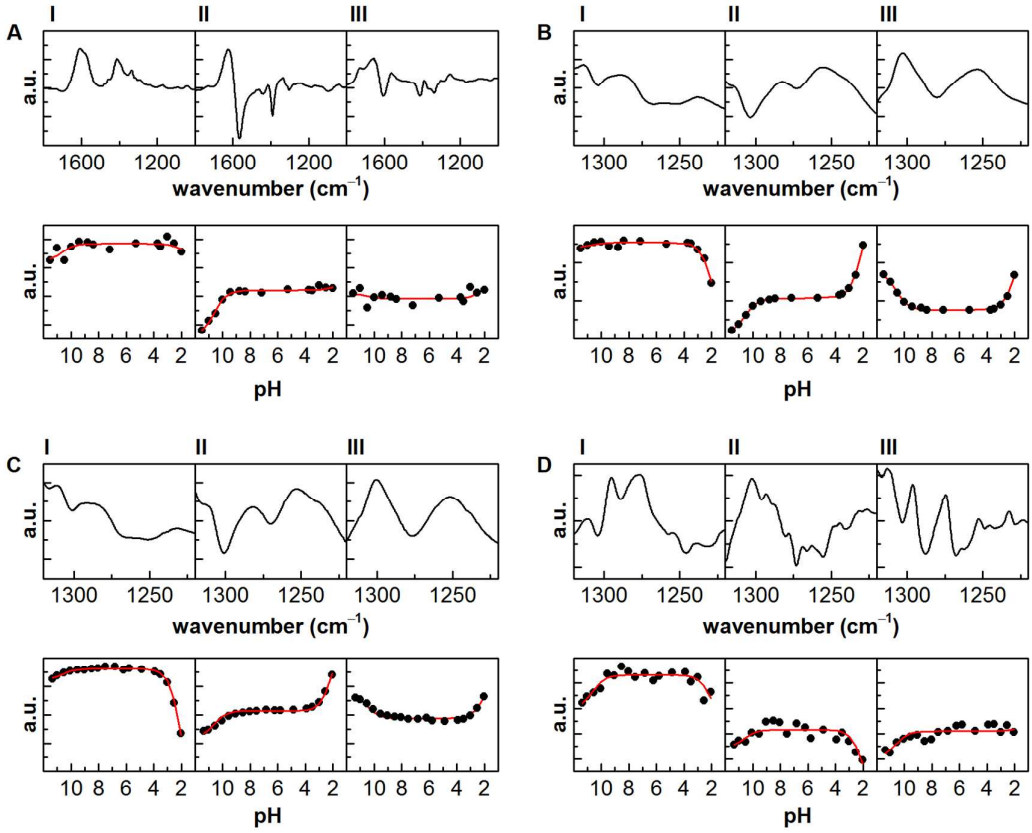

Figure S1. Orthonormal spectra (upper panels) and their associated orthonormal pH-titration vectors (lower panels) from SVD analysis of FT-IR data in the spectral range from 1800 to 1000 cm^{-1} (A), from 1320 to 1220 cm^{-1} (B), and QCL-IR (C) and QCL-VCD in the spectral range from 1320 to 1220 cm^{-1} (D). The first three orthonormal spectra in each panel confirm the existence of three significant components in each of the experimental data matrices. The orthonormal pH-titration vectors represent pH-titration curves for the corresponding SVD components (dots). Fitted curves using equation 3 (red lines) confirmed the suitability of the

two-pK Henderson–Hasselbalch equation to model the pH-dependence of spectral changes for the FT-IR, QCL-IR, and QCL-VCD data sets.

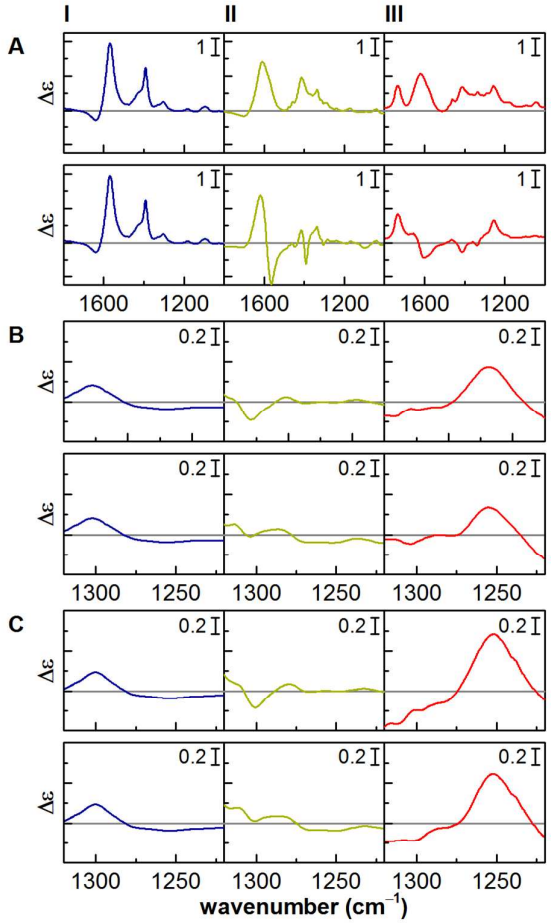

Figure S2. Amplitude spectra a_0 (I), a_2 (II), and a_1 (III) (upper panels) and pure spectra for anionic (= a_0, I), zwitterionic (= a_0 + a_2, II), and cationic (= a_0 + a_1 + a_2, III) L-proline from global fitting of FT-IR data (lower panels) in the spectral range from 1800 to 1000 cm^{-1} (A), from 1320 to 1220 cm^{-1} (B), and QCL-IR in the spectral range from 1320 to 1220 cm^{-1} (C).

QUANTUM CHEMICAL CALCULATIONS OF VCD SPECTRA

Anionic L-proline

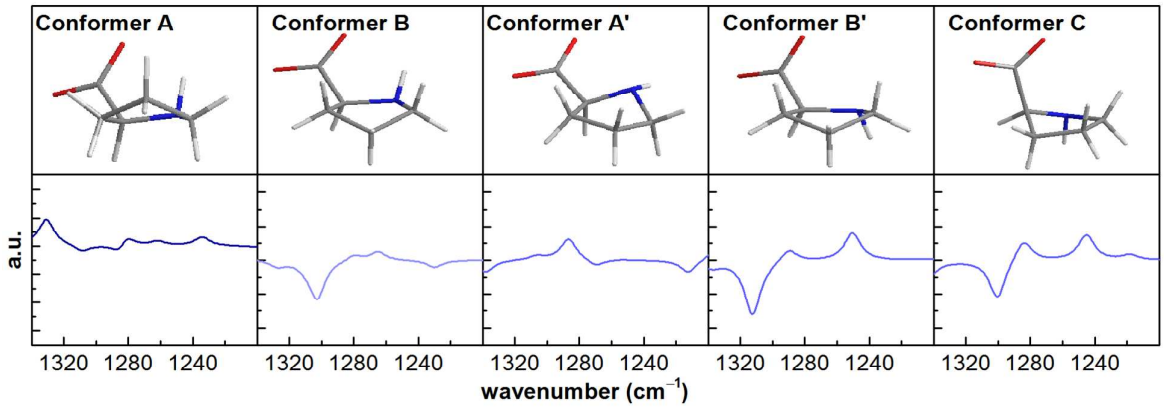

Figure S3. Conformers of anionic L-proline after geometry optimization and the corresponding VCD spectra calculated at the B3LYP/PCM/6-311++G(d,p) level. Conformers A and B were modeled by deprotonation of the nitrogen atom in conformers A and B, suggested by Kapitán et al. for zwitterionic L-proline.[3] The residual nitrogen-bound hydrogen atom has a *cis* orientation in respect to the carboxyl moiety, allowing for intramolecular interaction. Conformers A' and B' are conformers modeled with the opposite (*trans*) orientation of the hydrogen atom. Conformer C has also a *trans*-oriented hydrogen but different ring-puckering compared to A, B, A', and B'. C is a conformer previously obtained from gas phase calculations at the B3LYP/6-311++G(d,p) level for anionic L-proline[4] that does not interconvert into A, B, A', or B' after geometry optimization including implicit solvent by the use of a PCM.

Table S1: Relative energies and Boltzmann weights calculated fort the different conformers of anionic L-proline.

geometry	ΔE ($kJ \cdot mol^{-1}$)	Boltzmann weights (%) in respect to ΔE
A	0	61.29
B	1.19	37.75
A'	11.25	0.25
B'	13.46	0.63
C	16.42	0.08

Zwitterionic L-proline

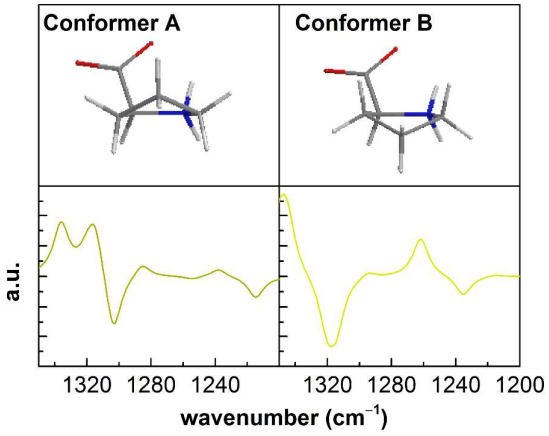

Figure S4. Conformers A and B of zwitterionic L-proline[3] after geometry optimization and the corresponding VCD spectra calculated at the B3LYP/PCM/6-311++G(d,p) level.

Table S2: Relative energies and Boltzmann weights calculated fort the different conformers of zwitterionic L-proline. The experimentally determined ratio A:B from NMR is about 50:50.[3]

geometry	ΔE (kJ·mol^{-1})	Boltzmann weights (%) in respect to ΔE
A	0	65.18
B	1.54	34.83

Cationic L-proline

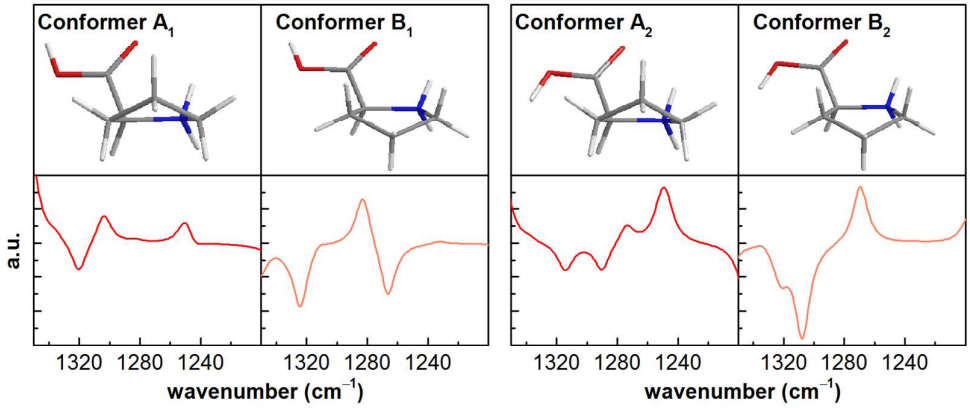

Figure S5. Conformers of cationic L-proline after geometry optimization and the corresponding VCD spectra calculated at the B3LYP/PCM/6-311++G(d,p) level. In cationic L-proline there exist additional conformers due to different orientations and rotamers of the O-H group.

Table S3. Relative energies and Boltzmann weights calculated fort the different conformers of cationic L-proline.

geometry	ΔE (kJ·mol^{-1})	Boltzmann weights (%) in respect to ΔE
A_1	0.57	44.03
A_2	14.45	0.16
B_1	0	55.60
B_2	14.71	0.22

REFERENCES

1. Shrager, R. I.; Hendler, R. W. Titration of Individual Components in a Mixture with Resolution of Difference Spectra, p*K*s, and Redox Transitions. *Anal. Chem.* **1982**, 54, 1147–1152.

2. Hendler, R. W.; Shrager, R. I. Deconvolutions Based on Singular-Value Decomposition and the Pseudoinverse: A Guide for Beginners. *J. Biochem. Bioph. Meth.* **1994**, 28, 1–33.

3. Kapitán, J.; Baumruk, V.; Kopecký, V.; Pohl, R.; Bouř, P. Proline Zwitterion Dynamics in Solution, Glass, and Crystalline State. *J. Am. Chem. Soc.* **2006**, 128, 13451–13462.

4. Marino, T.; Russo, N.; Tocci, E.; Toscano, M. Gas-Phase Acidity of Proline from Density Functional Computations. *Int. J. Quantum Chem.* **2001**, 84, 264-268.